Original Article

# Anterior segment optical coherence tomography evaluation of ocular graft-versus-host disease: a case study

**Peng Li[1], Yichen Sun[2,3], Sepideh Hariri[1], Zhehai Zhou[1], Yoshihiro Inamoto[4], Stephanie J. Lee[4], Tueng T. Shen[1,2], Ruikang K. Wang[1,2]**

[1]Department of Bioengineering, [2]Department of Ophthalmology, University of Washington, Seattle, WA 98195, USA; [3]Buddhist Tzu Chi General Hospital, Taipei Division, New Taipei, Taiwan; [4]Fred Hutchinson Cancer Research Center, Seattle, Washington 98109, USA

*Correspondence to:* Ruikang K. Wang. Department of Bioengineering, Department of Ophthalmology, University of Washington, Seattle, WA 98195, USA. Email: wangrk@uw.edu.

**Abstract:** To explore ocular graft-versus-host disease (GVHD), anterior segment optical coherence tomography (AS-OCT) imaging of eyelids, tear meniscus, cornea and conjunctiva is performed in subsequent sessions on a patient who has ocular GVHD after allogeneic related donor stem cell transplant. The OCT results are presented together with those from a normal subject. OCT imaging is promising in visualizing several ocular GVHD manifestations, such as abnormal meibomian gland orifice (MGO), conjunctival keratinization, conjunctival hyperemia and chemosis, corneal epithelium opacification, thinning and sloughing. This case study demonstrates the capability of AS-OCT in the imaging and monitoring of ocular GVHD, which may be useful in the development of current ocular GVHD staging system and the clinical management for GVHD treatment.

**Keywords:** Medical and biological imaging; optical coherence tomography (OCT); ophthalmology; ocular graft-versus-host disease (GVHD)

Submitted Sep 17, 2014. Accepted for publication Oct 20, 2014.
doi: 10.3978/j.issn.2223-4292.2014.11.05
**View this article at:** http://dx.doi.org/10.3978/j.issn.2223-4292.2014.11.05

## Introduction

Graft-versus-host disease (GVHD) is a major complication following allogeneic hematopoietic stem cell transplantation (aHSCT), occurring in 25-70% of patients, due to the reaction of transplanted immune cells against host's body cells (1-3). GVHD severely limits the full potential of aHSCT and is still one of the leading causes of morbidity and mortality in aHSCT.

Usually, GVHD involves several organ systems, such as skin, liver, gastrointestinal tract, mouth and eye (4,5). Among these target organs, ocular involvement occurs in ~60% of GVHD patients (1,3,4), and affects almost all parts of the eye, particularly cornea, conjunctiva, lids and lacrimal gland, resulting in a wide spectrum of ocular complications (1,2,5-8). Although ocular involvement is generally not a fatal problem, it has been well recognized that ocular GVHD causes considerable suffering and significantly impairs the quality of life (1-4,6-9).

The frequent and potentially severe ocular involvement in GVHD patients necessitates a full ocular evaluation (pre- and post-transplantation) of these patients for early recognition and timely treatment prior to the onset of other complications. Currently, the diagnosis of ocular GVHD is mainly based on the presence of ocular manifestations such as new-onset dry, gritty, or painful eyes, keratoconjunctivitis sicca, photophobia and punctate keratopathy, and is commonly confirmed by invasive biopsy or other relevant tests (5). Whereas, such clinical manifestations usually occur in a late phase of ocular GVHD and the recognition is more or less a subjective procedure. On the other hand, the invasive nature of biopsy precludes its use in the longitudinal assessment of disease progression and treatment response. Thus, a non-invasive examining method capable of detecting

**Table 1** Summary of clinical presentation of a ocular GVHD patient

| Age (years)/ Sex | Diagnosis | Period after transplantation | Ocular signs | OCT signs | Stage | Treatment |
|---|---|---|---|---|---|---|
| 55/Female | MDS | aHSCT, 9 months | PEE, filaments | • Abnormal MGO;<br>• Conjunctival keratinization;<br>• Conjunctival hyperemia with chemotic response;<br>• Corneal epithelium opacification, thinning & sloughing. | II | Bandage contact lens, topical lubricants, antibiotics |

GVHD, graft-versus-host disease; OCT, optical coherence tomography; MDS, myelodysplastic syndromes; aHSCT, allogeneic hematopoietic stem cell transplant; PEE, punctate epithelial erosion; MGO, meibomian gland orifice.

early changes is particularly attractive in the ocular GVHD.

In addition, a practical treatment guideline is necessary for diagnosing and treating ocular GVHD. Due to the frequent involvement of conjunctiva in the ocular GVHD, Jabs and his colleagues proposed a conjunctival GVHD staging system (8) and then refined with additional examination experience (4). This staging system mainly outlines the development of conjunctival GVHD. However, the involvement of other ocular GVHD manifestations is not considered. This is largely due to the current lack of appropriate assessment tools.

Optical coherence tomography (OCT) is an imaging tool capable of providing micrometer-resolution (<10 μm axial) cross-sectional and volumetric imaging of biological tissue in a non-contact, non-invasive and real-time fashion (10-12). Based on these attributes, OCT is considered particularly suited for ocular imaging and is currently part of the clinical standard of patient care in ophthalmology.

The aim of this pilot case study is to explore the feasibility of using OCT to better evaluate ocular GVHD. Based on the common manifestations of ocular GVHD, the OCT imaging is mainly focused on four regions of interests (ROIs), including conjunctiva, cornea, eyelids and tear meniscus.

## Materials and methods

The study was approved by the Institutional Review Board at the Fred Hutchinson Cancer Research Center and the University of Washington. The patient was recruited with prior informed consent. Information from the GVHD patient with ocular involvement is summarized in *Table 1*. OCT imaging was performed prior the bandage contact lens trial (GVHD0), and then two follow-up examinations at 2-week interval were performed for assessing treatment response (GVHD2 & GVHD4).

We used an anterior segment OCT (AS-OCT) system in this study. The system was reported in detail in reference (13), except the light source employed. The light source was a broadband superluminescent diode (SLD) with a central wavelength of 1,340 nm and a spectral bandwidth of 110 nm, providing an axial resolution of ~7.2 μm in air. An objective lens with a 50 mm focal length was used in the sample arm to deliver the probing light to the ROIs at the cornea, yielding a measured lateral resolution of ~16 μm. A brief schematic representation of the OCT system is presented in *Figure 1*.

We focused OCT imaging on four selected ROIs including eyelid, tear meniscus, cornea and conjunctiva. Specifically, for eyelids and tear menisci, the OCT imaging was performed at the inferior portion of the eye, while for cornea it was at the central cornea. The scanning protocol was optimized for real-time, high-definition microstructural imaging, in which the data volume consists of 512 (depth pixels) × 512 (A lines) × 512 (B-frames) covering 3×4.5×4.5 $mm^3$ that required an acquisition time of ~3.6 seconds. For conjunctival region, the OCT imaging was performed at the nasal portion of eye. This later scanning protocol was optimized for imaging microstructure, blood and lymphatic vasculature in parallel as detailed in reference (14). The data volume consists of 512 (depth pixels) × 360 (A lines) × 1,000 (B-frames) covering 3×4.5×4.5 $mm^3$ that required an acquisition time of ~5 seconds. The 1,000 B-frames was captured 200 sampling positions with five repeated scans at each position in order to achieve the imaging of blood perfusion within conjunctival tissue beds by the use of optical microangiography (OMAG) (15-18). In addition, because the lymphatic vessel lumen appears as low-signal region in the OCT image, a semi-automatic segmentation software (19) was use to segment the three dimensional (3D) lymphatic vasculatures out from the surrounding structures (20,21).

 

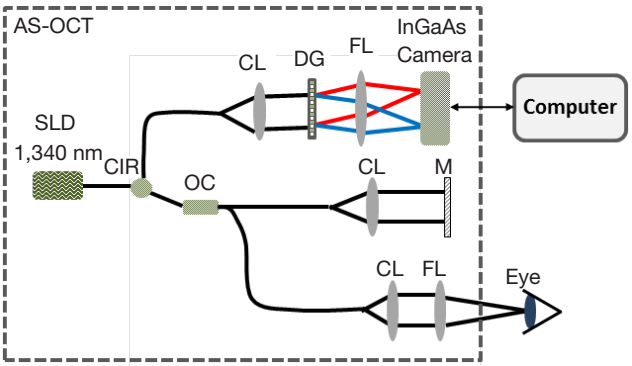


**Figure 1** Schematic diagram of the anterior segment optical coherence tomography (AS-OCT) system including superluminescent diode (SLD); circulator (CIR); optical coupler (OC); collimating lens (CL); focusing lens (FL); diffraction grating (DG); mirror (M).

## Results

### *Normal subject (Figures 2-5)*

A normal subject was scanned by AS-OCT as well. The protocol of the normal subject was similar to the study patient. The representative results were respectively reported in *Figure 2A2*, *A3*, *Figure 3B*, *Figure 4A* and *Figure 5A1* for comparing with GVHD data.

### *GVHD case*

A 55-year-old woman with myelodysplastic syndrome (MDS) who underwent aHSCT in December 2011 suffered from severe photosensitivity and gritty sensation since May 2012. Bilateral diffuse punctate epithelial erosions (PEEs)

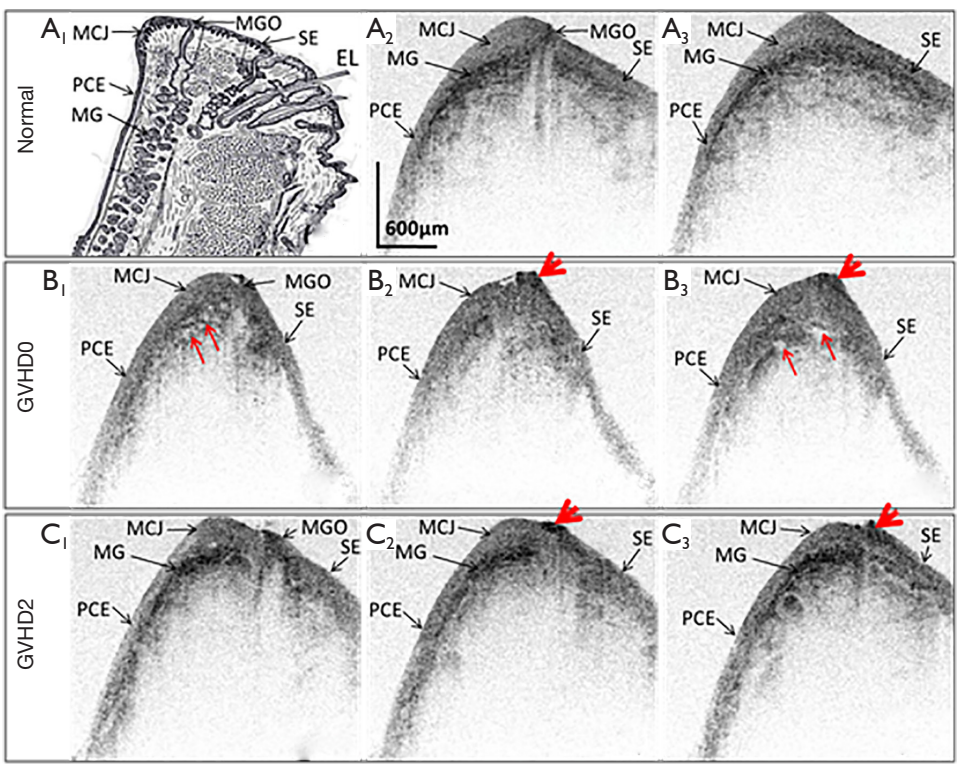


**Figure 2** Inverted OCT images at the lower eyelid. Rows (A), (B) and (C) report the representative OCT cross-sections of lower eyelid from a normal subject, an ocular GVHD patient at her first visit before treatment (baseline, GVHD0) and at 2-week follow-up visit (GVHD2), respectively. (A1) Schematic of eyelid; (A2) eyelid OCT cross-section through MGO. MGO is visible. MG appears as a high-scattering region beneath PCE and MCJ; (A3) eyelid OCT cross-section of MGO; (B1) eyelid OCT cross-section through a MGO. MGO is less visible. MG is inflamed and appears as low-scattering regions indicated by thin red arrows; (B2) and (B3) eyelid OCT cross-section around MGO. High-scattering scar appears at around MGO, as marked by bold red arrows; (C1) eyelid OCT cross-section through a MGO. MGO is still less visible. MG inflammation gets somewhat relieved; (C2) and (C3) eyelid cross-section around MGO. High-scattering scar still appears around MGO. SE, skin epidermis; PCE, palpebral conjunctival epithelium; MCJ, mucocutaneous junction; MGO, meibomian gland orifice; MG, meibomian gland; EL, eyelash; OCT, optical coherence tomography; GVHD, graft-versus-host disease.

 

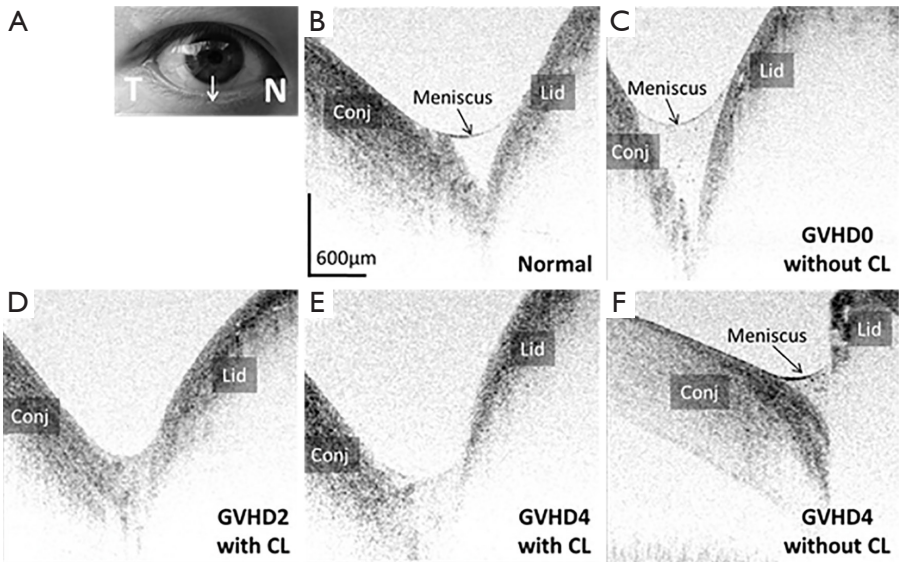


**Figure 3** OCT provides ability to delineate the lower tear meniscus. (A) Photo of human eye. The arrow illustrates the OCT scanning position for imaging the tear meniscus; (B) OCT cross-section of lower tear meniscus of a normal subject. Tear meniscus is clear and transparent; (C) OCT cross-section of the lower tear meniscus of ocular GVHD patient at the first visit before treatment (baseline, GVHD0), no contact lens. Tear meniscus is visible but turbid; (D) the lower tear meniscus, 2-week follow-up visit (GVHD2), wearing contact lens. Less tear meniscus is evident; (E) lower tear meniscus, 4-week follow-up visit (GVHD4), wearing contact lens. Tear meniscus is still less; (F) lower tear meniscus, 4-week follow-up visit (GVHD4), no contact lens. Tear meniscus I present, but turbid. T, temporal; N, nasal; Conj, conjunctiva; Lid, eyelid; GVHD, graft-versus-host disease; CL, contact lens; OCT, optical coherence tomography.

and a few corneal filaments were disclosed at her first visit to ophthalmic clinic. A series of AS-OCT imaging were taken after ocular examination. The AS-OCT images acquired from the normal subjects indicate that OCT is able to delineate meibomian gland orifice (MGO) (*Figure 2A2*), and the meibomian gland (MG) appears as a high-scattering region beneath palpebral conjunctival epithelium (PCE) and mucocutaneous junction (MCJ) (*Figure 2A2*,*A3*). However, the OCT images acquired from the ocular GVHD patient showed less visible MGO than normal subjects, and there appeared some scarring-like tissue around MGO in her first two visits (before treatment, GVHD0, *Figure 2B* and 2-week follow-up visit, GVHD2, *Figure 2C*). In addition, the MG was presented more inflamed and appeared as low-scattering regions in the OCT images acquired at her first visit (*Figure 2B*); however, this inflammation was somewhat relieved at her 2-week follow-up visit (*Figure 2C*). The image appearance of eyelid at her 4-week follow-up visit was almost the same as her 2-week follow-up visit (GVHD2).

In contrast to its clear and transparent appearance in normal subjects (*Figure 3B*), the tear meniscus in the GVHD patient was visiblely turbid at the first visit prior to treatment (*Figure 3C*). During the 2-week and 4-week follow-up visits, tear meniscus significantly reduced while wearing contact lens (*Figure 3D*,*F*). After taking off contact lens at the 4-week follow-up visit, the turbid tear meniscus appeared again in OCT cross-sectional image (*Figure 3F*).

As shown in *Figure 4*, compared to the normal subject (refer to *Figure 4A*,*A2*), the corneal epithelium of the GVHD patient showed less transparency, mild opacity and high scattering with less smooth corneal surface at her first visit prior to treatment (refer to *Figure 4B*). Bilateral bandage contact lenses were placed after the first ocular examination. The patient was also received topical antibiotics and lubricants at the time of imaging. During the 2-week and 4-week follow-up visits (refer to *Figure 4C*,*D*,*D1*), the OCT images indicate that the original less-transparent corneal epithelium becomes thinned and sloughing in the region marked by the star in *Figure 4A1*, which might be lightly scraped off by contact lens clinically.

As reported in *Figure 5*, compared to that of normal subject (*Figure 5A1*), the conjunctival image of GVHD shows much higher OCT signal on the surface which is most likely due to the conjunctival keratinization. In

 

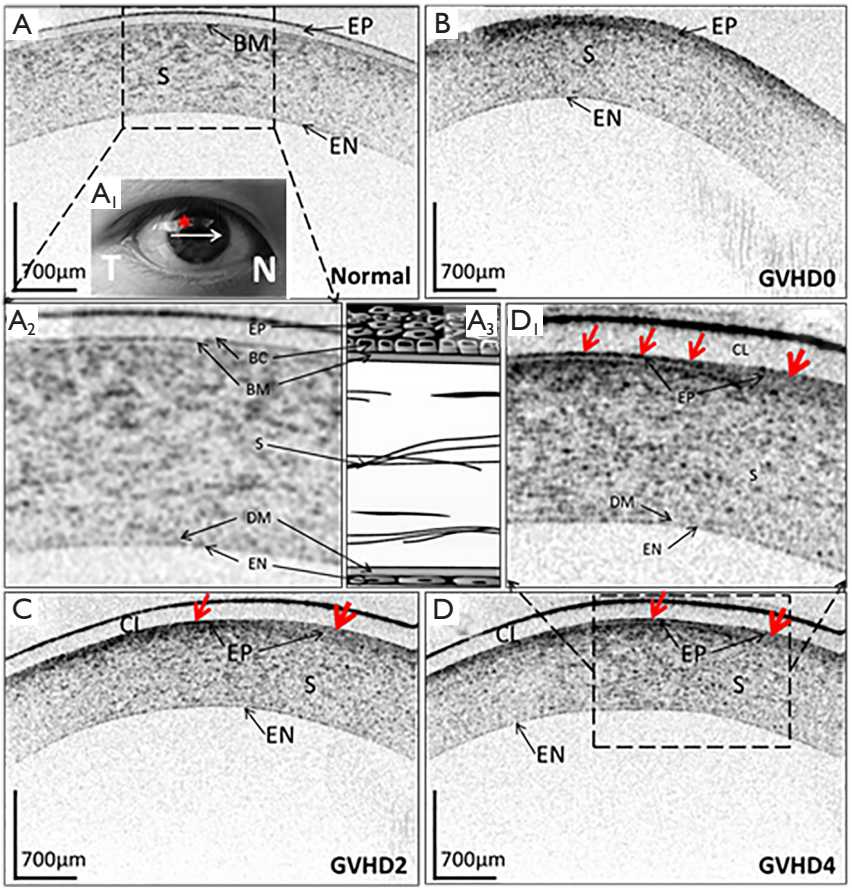


**Figure 4** OCT imaging of the cornea. (A) Representative corneal OCT cross-section of the normal subject. Epithelium is transparent; (A1) photo of human eye. White arrow shows the OCT scanning position for corneal imaging; (A2) enlarged view of the region marked in (A) by dashed square; (A3) schematic of layered structure of cornea; (B) baseline of cornea from ocular GVHD patient at the first visit before treatment (termed as GVHD0). Epithelium is less transparent while increased opacity and high scattering is observed. The corneal surface is less smooth; (C) and (D) corneal cross-section from the GVHD case respectively at 2-week follow-up visit (GVHD2) and at 4-week follow-up visit (GVHD4). Epithelium gets thinned in the region marked by the star in (A1) (comparing the region indicated by bold red arrows and by thin red arrows); (D1) enlarged view of the region marked in (D) by dashed square. The less-transparent epithelium is thinning and sloughing, which can be readily scraped off clinically. T, temporal; N, nasal; EP, epithelium; BC, basal cell layer; BM, Bowman's membrane; S, stroma; DM, Descemet's membrane; EN, endothelium; CL, contact lens; GVHD, graft-versus-host disease; OCT, optical coherence tomography.

addition, the conjunctival lymphatic vessels are dilated in GVHD patient compared to those in normal subject (as marked by stars in *Figure 5B1*,*C1*,*D1*). And the chemotic response can be observed around the boundary between conjunctiva and sclera (as indicated by thin arrows in *Figure 5B1*,*B3*,*C3*,*D1*,*D3*). Based on the 3D conjunctival OCT images, the lymphatic vasculature and chemosis can be differentiated from the surrounding tissues, as shown by the depth-encoded projection views in *Figure 5B2*,*C2*,*D2*, where the yellow and orange colors are primarily corresponding to chemosis, and blue and green colors are mainly corresponding to lymphatic vessels. It is noticed that much more obvious conjunctival chemosis was present at the first visit prior to treatment, and it was reduced significantly during the 2-week and 4-week follow-up visits after adequate treatment. However, the conjunctival hyperemia still existed at her 4-week follow-up visit (*Figure 6*) as shown by the dense blood vasculature in *Figure 6D*.

## Discussion and conclusions

Non-invasive OCT imaging findings in our patient

 

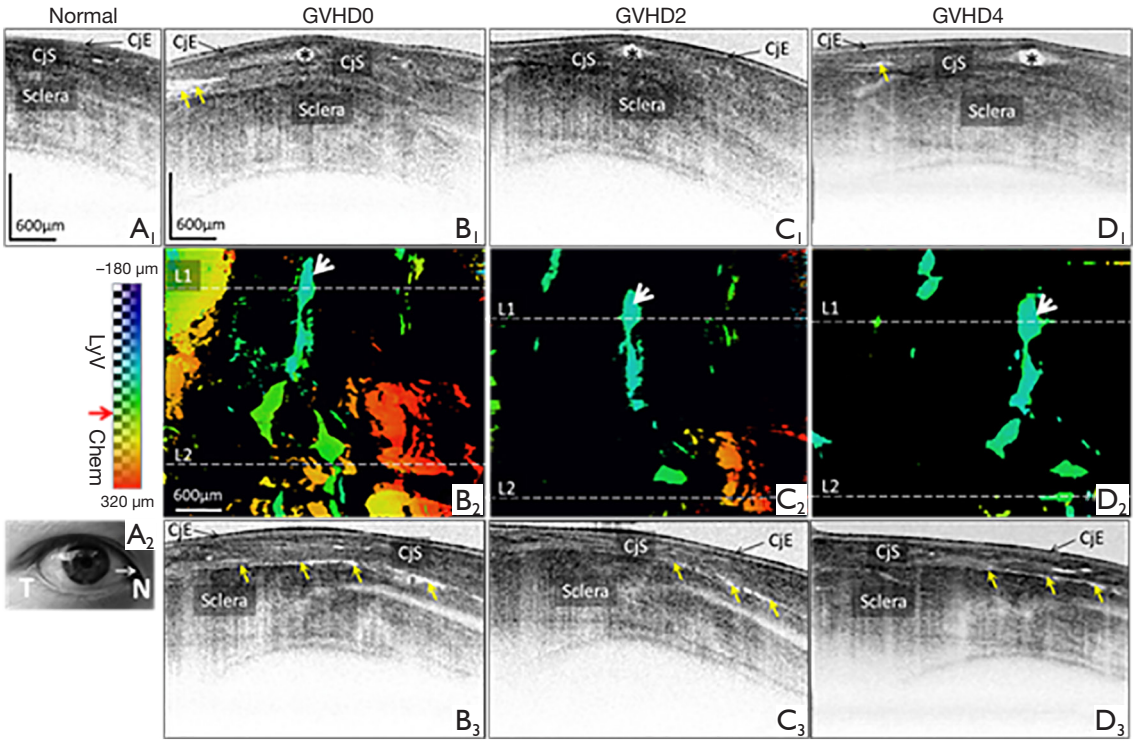


**Figure 5** OCT imaging of conjunctiva. (A1) Representative conjunctival OCT cross-section of the normal subject; (A2) photo of human eye. Red arrow shows the OCT scanning position for conjunctival imaging; Columns (A), (B) and (C) report the conjunctiva of GVHD at the first visit before treatment (baseline, GVHD0), at 2-week follow-up visit (GVHD2) and at 4-week follow-up visit (GVHD4), respectively; figures in row 2 report the projection views of depth-encoded lymphatic vessels and chemosis which are segmented from the 3D micro-structural imaging. The superficial layer corresponds to LyV and the deeper layer corresponds to Chem, as shown by the color bar. Bold white arrows indicate a big lymphatic vessel; rows 1 and 3 respectively illustrate the cross-sections along the dashed lines L1 and L2 in row 2. The stars mark the lymphatic vessel, and the thin arrows indicate the chemosis. CjE, conjunctival epithelium; CjS, conjunctival stroma; LyV, lymphatic vessels; Chem, chemosis; T, temporal; N, nasal; GVHD, graft-versus-host disease; OCT, optical coherence tomography; 3D, three dimensional.

showed scar formation of the MGO (*Figure 2*), confirming the clinical observations on ocular GVHD patients. It is known that the tear film, which plays an important role in maintaining ocular surface and clear vision, is mainly composed of three physiological layers: lipid layer by MG, aqueous layer by lacrimal gland and mucin layer by conjunctival goblet cells. Our findings on the tear meniscus (*Figure 3*) demonstrated a different relationship between the tear production and severity of ocular surface pathology as currently characterized by Schirmer's test (measuring tear production): we observed higher tear meniscus during the initial exam while the ocular surface irritation caused reflex tearing, in contrast to the conventional believe that GVHD patients lacks tears. This further confirmed that Schirmer's test, the current standard for ocular GVHD staging, has not been accurate in correlating with clinical findings.

According to the results of this pilot study, we found MG dysfunction possibly appears at the early stage, affecting the lipid/oil secretion, while the tear/aqueous secretion by lacrimal gland is still functioning. The lack of the MG secretions would accelerate the evaporation of tear film and influence the functions of tear film, which together might be responsible for the above-mentioned disorders of cornea (refer to *Figure 4*) and conjunctiva (refer to *Figures 5,6*). Our non-invasive *in vivo* imaging in GVHD patient has demonstrated for the first time the inflammatory changes of the ocular surface vasculartur and chemosis in response to treatment with bandage contact lenses. AS-OCT offers unique advantage of precise dynamic analysis of the ocular surface system without physical disturbance (compared to Schirmer's). This information will be invaluable for the fundimental understanding of the pathophysiology of the GVHD.

 

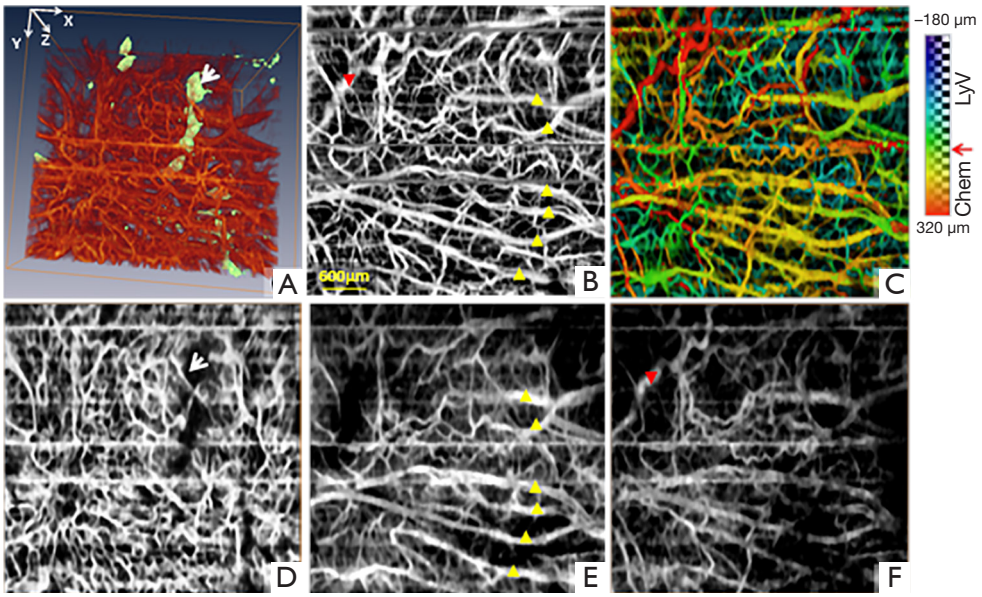


**Figure 6** Optical micro-angiography (OMAG) of conjunctiva from the GVHD case at 4-week follow-up visit (GVHD4). (A) 3D rendering of the merged blood perfusion and lymphatic vasculature; (B) projection view (x-y) from the 3D blood flow image; (C) depth-encoded projection view in (B); (D), (E) and (F) en-face blood flow imaging at conjunctiva, episcleral and intrascleral. The bold white arrow indicates the same lymphatic vessel as shown in *Figure 5* (*D2*). The yellow upward triangles indicate the episcleral vessels, and the red downward triangles indicate the intrascleral vessels. The color bar ranges from -180 μm to 320 μm. Negative value indicates a distance above eye surface, and positive value implies a distance below eye surface. LyV, lymphatic vessels; Chem, chemosis; GVHD, graft-versus-host disease; 3D, three dimensional.

Referring to the ocular GVHD conjunctival staging system proposed by Jabs *et al*. (8) and combining with the clinical manifestations, this ocular patient is most likely corresponding to stage II GVHD.

"The earlier the detection, the better the prognosis would be". Ocular GVHD is also one of the ocular surface disorders that follow this rule. The promising results from this pilot case study demonstrates the feasibility of using OCT for ocular GVHD examination at early stages. The detailed information extracted from OCT, including MG, tear film, corneal epithelium, and conjunctival vasculature, can potentionally be used for enriching the current ocular GVHD staging system and the clinical management for GVHD treatment. In the future, more pre- and post-aHSCT with or without ocular GVHD cases will be recruited for OCT imaging and statistical analysis to investigate the significance between these reported OCT findings and ocular GVHD.

## Acknowledgements

This work was supported in part by the Lions Research Fund, the Guiliani Family Foundation, Research to Prevent Blindness and the Coulter translational research grant.

*Disclosure:* The authors declare no conflict of interest.

## References

1. Franklin RM, Kenyon KR, Tutschka PJ, Saral R, Green WR, Santos GW. Ocular manifestations of graft-vs-host disease. Ophthalmology 1983;90:4-13.
2. Jack MK, Jack GM, Sale GE, Shulman HM, Sullivan KM. Ocular manifestations of graft-v-host disease. Arch Ophthalmol 1983;101:1080-4.
3. Anderson NG, Regillo C. Ocular manifestations of graft versus host disease. Curr Opin Ophthalmol 2004;15:503-7.
4. Riemens A, te Boome L, Imhof S, Kuball J, Rothova A. Current insights into ocular graft-versus-host disease. Curr Opin Ophthalmol 2010;21:485-94.
5. Filipovich AH. Diagnosis and manifestations of chronic graft-versus-host disease. Best Pract Res Clin Haematol 2008;21:251-7.

 

6. Hirst LW, Jabs DA, Tutschka PJ, Green WR, Santos GW. The eye in bone marrow transplantation. I. Clinical study. Arch Ophthalmol 1983;101:580-4.
7. Jabs DA, Hirst LW, Green WR, Tutschka PJ, Santos GW, Beschorner WE. The eye in bone marrow transplantation. II. Histopathology. Arch Ophthalmol 1983;101:585-90.
8. Jabs DA, Wingard J, Green WR, Farmer ER, Vogelsang G, Saral R. The eye in bone marrow transplantation. III. Conjunctival graft-vs-host disease. Arch Ophthalmol 1989;107:1343-8.
9. Kim SK. Update on ocular graft versus host disease. Curr Opin Ophthalmol 2006;17:344-8.
10. Huang D, Swanson EA, Lin CP, Schuman JS, Stinson WG, Chang W, Hee MR, Flotte T, Gregory K, Puliafito CA, Fujimoto JG. Optical coherence tomography. Science 1991;254:1178-81.
11. Tomlins PH, Wang RK. Theory, developments and applications of optical coherence tomography. J Phys D: Appl Phys 2005;38:2519.
12. Fercher AF, Drexler W, Hitzenberger CK, Lasser T. Optical coherence tomography - principles and applications. Rep Prog Phys 2003;66:239.
13. Li P, Johnstone M, Wang RK. Full anterior segment biometry with extended imaging range spectral domain optical coherence tomography at 1340 nm. J Biomed Opt 2014;19:046013.
14. Li P, An L, Reif R, Shen TT, Johnstone M, Wang RK. In vivo microstructural and microvascular imaging of the human corneo-scleral limbus using optical coherence tomography. Biomed Opt Express 2011;2:3109-18.
15. Wang RK, Jacques SL, Ma Z, Hurst S, Hanson SR, Gruber A. Three dimensional optical angiography. Opt Express 2007;15:4083-97.
16. Wang RK, An L, Francis P, Wilson DJ. Depth-resolved imaging of capillary networks in retina and choroid using ultrahigh sensitive optical microangiography. Opt Lett 2010;35:1467-9.
17. An L, Qin J, Wang RK. Ultrahigh sensitive optical microangiography for in vivo imaging of microcirculations within human skin tissue beds. Opt Express 2010;18:8220-8.
18. Reif R, Wang RK. Label-free imaging of blood vessel morphology with capillary resolution using optical microangiography. Quant Imaging Med Surg 2012;2:207-12.
19. Yin X, Chao JR, Wang RK. User-guided segmentation for volumetric retinal optical coherence tomography images. J Biomed Opt 2014;19:086020.
20. Yousefi S, Qin J, Zhi Z, Wang RK. Label-free optical lymphangiography: development of an automatic segmentation method applied to optical coherence tomography to visualize lymphatic vessels using Hessian filters. J Biomed Opt 2013;18:86004.
21. Yousefi S, Zhi Z, Wang RK. Label-free optical imaging of lymphatic vessels within tissue beds in vivo. IEEE J Sel Top Quantum Electron 2014;20:6800510.

**Cite this article as:** Li P, Sun Y, Hariri S, Zhou Z, Inamoto Y, Lee SJ, Shen TT, Wang RK. Anterior segment optical coherence tomography evaluation of ocular graft-versus-host disease: a case study. Quant Imaging Med Surg 2015;5(1):163-170. doi: 10.3978/j.issn.2223-4292.2014.11.05

 